

# Gamut expanded halftone prints

Romain Rossier, Roger D. Hersch, School of Computer and Communication Sciences, Ecole Polytechnique Fédérale de Lausanne (EPFL), Switzerland

## Abstract

*We propose a framework for printing high chroma and bright colors which are beyond both the display sRGB and the classical cmyk print gamuts. These colors are printed with a combination of classical cmyk inks and the two additional daylight fluorescent magenta and yellow inks. The goal is to enhance image parts by printing them with high chroma and bright colors. We first select the image parts to be enhanced. We then apply to their colors a gamut expansion that increases both their chroma and their lightness towards the colors located at the boundary of the gamut formed by the combination of classical and fluorescent inks. This expansion can be controlled by user-defined parameters. We create smooth chroma transitions between the expanded and non-expanded image parts. We also preview the printable gamut expanded image generated according to user-defined gamut expansion parameters. The resulting prototype software enables artists to create and print their own designs.*

## Introduction

In the present contribution, we generate gamut expanded images by printing colors located beyond the display sRGB gamut using a six ink printing system combining the classical cmyk inks with the daylight fluorescent magenta and yellow inks. Daylight fluorescent colorants are widely used in products that aim at capturing the attention of human such as highlighting markers, safety jackets and traffic signs. Fluorescent brighteners are used as whitening agents in tissues and paper. We would like to use the possibilities offered by the high chroma and bright daylight fluorescent colors in order to highlight image regions of special interest. Highlighted image parts are printed with colors beyond the sRGB gamut while the remaining image parts are printed with colors present within the sRGB gamut.

We establish the total fluorescent  $G_f$  gamut by the conjunction of fluorescent sub-gamuts formed by classical inks with one or two daylight fluorescent inks. We use multiple strategies for mapping the input display sRGB gamut  $G_{sRGB}$  onto the printable destination gamut  $G_f$ . These multiple mapping strategies define how input image  $G_{sRGB}$  gamut colors are expanded to colors beyond the  $G_{sRGB}$  gamut while preserving the overall aesthetics of the input image.

We created specific tools for exploiting the capabilities of the expanded  $G_f$  gamut. They enable selecting an input image, applying to specific regions of that image different gamut expansions, displaying a preview and printing of the resulting gamut expanded printable image. The application offers new means for designers working in fields such as photography, advertisement and magazine production.

Producing gamut expanded images raises several challenges. We have to determine expansion factors increasing the chroma of input sRGB colors to colors beyond the sRGB gamut and possibly modify their lightness. The goal is to enhance given image parts with higher chroma and brighter colors. We also have to ensure the continuity of colors at the boundary between highlighted and non-highlighted image regions. In addition, we have to generate halftoned images comprising at different locations different gamut mappings between the input image and the destination image. In order to preview the printable highlighted images having colors beyond the sRGB gamut, we simulate a lower quality display for classical image parts and render the extended sRGB colors by making use of the full capabilities of the display. Such a preview enables visualizing the differences between the color expanded and non-expanded image parts. In order to compute ink surface coverages yielding the desired colors, we need to create a model predicting accurately the color of halftones comprising daylight fluorescent inks. Then, for printing a given expanded or non-expanded color we need to select an adequate set of 3 or 4 inks from the six available inks. Fading of the daylight fluorescent inks [10] can be limited by printing thick ink layers and/or by coating the printed layers with a UV-absorbing coating [9]. Ink manufacturers are developing fading resistant daylight fluorescent pigments.

## Related work

Guyler [1] compared the gamuts of classical and combined classical and daylight fluorescent inks for offset prints by relying on Neugebauer primaries and on printed color patch measurements. In a previous publication [2], Rossier and Hersch proposed to reproduce color images by combining classical and daylight fluorescent inks by using a spectral prediction model predicting the spectral reflectances of halftones comprising daylight fluorescent inks, a gamut mapping scheme from display gamut to the fluorescent printer gamut, and a color separation of the 6 ink layers. The proposed solution was however limited to gamut reduction from display  $G_{sRGB}$  gamut to the gamut  $G_f$  offered by the fluorescent inks. No gamut expansion beyond the  $G_{sRGB}$  gamut was foreseen.

Printing with combined classical and daylight fluorescent inks custom ink faces similar problems as printing with custom inks. There is a need to select a specific subset of inks from many possible ink subsets and to map the input gamut into the gamut achievable with multi-ink halftones. Stollnitz, Ostromoukhov and Salesin modeled the gamut of printable custom colorants by a modified Neugebauer model accounting for trapping, dot gain and multiple internal reflectances. With this model, they optimized the selection of custom inks in order to obtain a given color [3]. Tzeng and Berns used cyan,

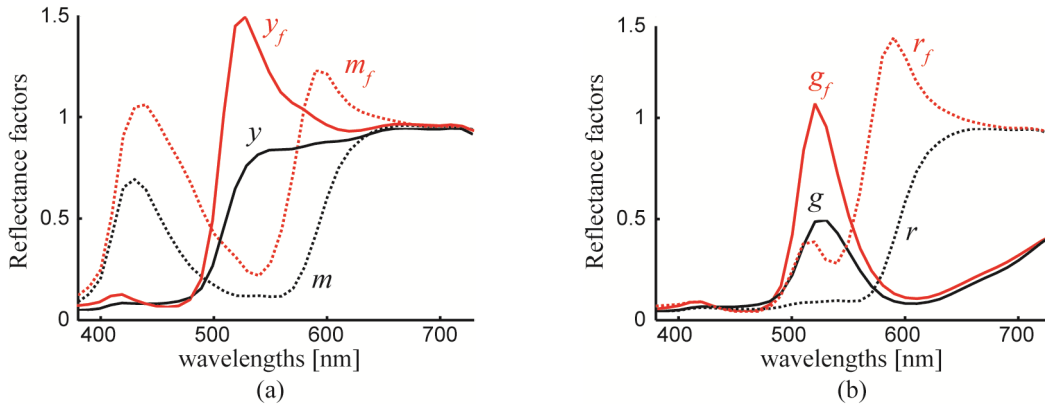


**Figure 1.** Reflectance factors under the D65 illuminant of (a) the daylight fluorescent  $m_f$  and  $y_f$  colorants and (b) the daylight fluorescent green (cyan superposed with  $y_f$ ) and red ( $m_f$  superposed with  $y_f$ ) colorants (red lines), together with the classical original Epson P50 colorant reflectances (black lines), printed on a fluorescent paper containing optical brighteners (Canon MP-101).

magenta, yellow, black, orange and green inks and developed an algorithm for selecting a subset of 4 inks among the 6 inks to reproduce a given reflection spectrum as accurately as possible, i.e. by minimizing metamerism [4].

Byoung-Ho Kand et. al. performed a user study which in addition to gamut compression also dealt with users performing interactive gamut expansion from print gamut to display gamut [11]. For most colors, besides memory colors, the users tried to extend the chroma of the images. Toyoshi Morioka et. al. showed that, compared with linear expansion, non-linear chroma expansion of *sRGB* images displayed on a wide gamut Adobe *RGB* monitor was preferred by users [14].

### Framework for printing daylight fluorescent inks

By combining the daylight fluorescent magenta ( $m_f$ ) and yellow ( $y_f$ ) inks with classical inks, we can create high chroma and bright colors. Figure 1 shows the total spectral reflectance factors [5] of four daylight fluorescent colorants together with the classical colorant reflectances, measured under a D65 illuminant by a SpectroEye Gretag-Macbeth spectrophotometer. Due to the fluorescence of the  $m_f$  and  $y_f$  inks, these colorants have a significantly higher chroma and are brighter than the corresponding classical colorants. They allow enhancing the chroma and lightness of parts of the printable images.

Let us establish the framework for printing with combinations of daylight fluorescent and classical inks. For this purpose, we establish the *sRGB* gamut  $G_{sRGB}$  and the print fluorescent gamut  $G_f$ . The fluorescent gamut comprises all colors printable with cyan, magenta, yellow, black, fluorescent magenta ( $m_f$ ) and fluorescent yellow ( $y_f$ ). We map the  $G_{sRGB}$  gamut into the  $G_f$  gamut by gamut expansions allowing to print beyond  $G_{sRGB}$  gamut colors. Mapping the *sRGB* gamut into the fluorescent ink gamut [8] requires (a) mapping the lightness range of the *sRGB* gamut into the lightness range of the fluorescent ink gamut by lightness adaptation, (b) creating the volume of the lightness adapted *sRGB* gamut and of the printable fluorescent gamut  $G_f$  and (c) mapping the lightness adapted *sRGB* gamut into the printable fluorescent gamut

according to user-defined chroma reduction and expansion factors. Thanks to chroma expansion, original image colors may be mapped into high chroma colors partially located outside the *sRGB* gamut, thereby highlighting the considered image parts.

### Mapping the lightness range of the *sRGB* gamut into the ink destination gamut

In order to map the  $G_{sRGB}$  lightness range into the destination gamut lightness range, we first determine the minimal lightness  $L^*_{inksMin}$  of the inks, i.e. the lightness of the solid pure black ink. We may then either apply a linear mapping that better preserves lightness differences of the input *sRGB* image space but raises all *sRGB* lightnesses, apply a partly non-linear mapping that preserves high lightness values but maps low lightnesses into a smaller lightness range or apply an s-shape like non-linear mapping. These lightness mappings can be defined with a cubic Bézier function

$$B(t) = (1-t)^3 P_0 + 3(1-t)^2 t P_1 + 3(1-t) t^2 P_2 + t^3 P_3 \quad t \in [0,1] \quad (1)$$

where  $P_0, P_4$  are the points  $(0, L^*_{inksMin}), (100, 100)$ , and where parameter  $t$  is varied between zero and one.

Control points  $P_1$  and  $P_2$  are user-defined according to the type of mapping. In case of a linear lightness mapping, the control points  $P_1$  and  $P_2$  are respectively set to  $(0, L^*_{inksMin})$  and  $(100, 100)$  (Fig. 2, solid line). In case of a partly non-linear mapping,  $P_1$  and  $P_2$  are both set to  $(L^*_{inksMin}, L^*_{inksMin})$ . This preserves lightnesses for  $L^* > 50$  (Fig. 2, dashed line). In case of a s-shaped non-linear mapping, lightnesses between  $L^* = 50$  and  $L^* = 60$  are preserved, but raised at lightnesses  $L^* > 60$ . Control points  $P_1$  and  $P_2$  can for instance be set to  $(2 \cdot L^*_{inksMin}, L^*_{inksMin})$  and  $(80, 100)$  (Fig. 2, pointed line).

The linear lightness mapping better preserves lightness differences present in the original input image. This yields for a wide range of input images the better printed reproductions. We therefore consider only linear lightness range mapping for the examples presented in this contribution.

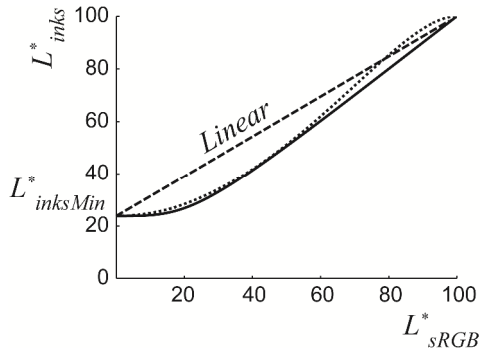


**Figure 2.** Linear (dashed line) and non-linear mapping of *sRGB* lightnesses. For the non-linear mapping, the input *sRGB* lightness values are either non-linearly mapped between  $L^* = 0$  and  $L^* = 50$  and preserved beyond  $L^* = 50$  (solid line) or preserved between  $L^* = 50$  and  $L^* = 60$  and shifted to higher values beyond  $L^* = 60$  (pointed lines).

### Establishing the lightness adapted *sRGB* gamut and the printable fluorescent gamut

The ink spreading enhanced cellular Yule-Nielsen spectral prediction model (IS-CYNSN) [6] is remarkably accurate for predicting the spectral reflectances of halftones comprising daylight fluorescent inks. It achieves a mean prediction error of  $\Delta E_{94}$  of 0.7 when predicting the total spectral reflectances of 125 uniformly distributed halftones comprising at least one daylight fluorescent ink. Accurate spectral predictions are needed for establishing the printable destination fluorescent gamut as well as for creating a correspondence between CIELAB colors and corresponding fluorescent ink dot surface coverages.

The printable fluorescent gamut  $G_f$  is the conjunction of the four  $cm\beta_f$ ,  $cm\beta$ ,  $cm\gamma$  and  $cm\gamma$  ink set sub-gamuts, i.e. one color of the total printable fluorescent gamut  $G_f$  is located within at least one of these sub-gamuts and is printed with its corresponding inks. We halftone the individual ink layers with a blue noise dispersed dither halftoning algorithm. This prevents the occurrence of artifacts at the boundaries between halftones produced with non-fluorescent and with fluorescent ink sets. The  $G_f$  gamut is established by predicting with the IS-CYNSN spectral prediction model the total reflectance factors of halftones by varying nominal ink surface coverages by small steps for the 4 ink sets  $cm\gamma$ ,  $cm\beta_f$ ,  $cm\beta$  and  $cm\gamma$ , by converting them to CIE-XYZ tri-stimulus values under the D65 illuminant and by computing the corresponding CIELAB colors. The non-convex  $G_f$  gamut boundary is obtained by performing a Delaunay triangulation of the CIELAB color points and by computing with the Ball-Pivoting algorithm [7] the set of surface triangles forming the concave boundary. The lightness adapted *sRGB* gamut is obtained by varying the *sRGB* red, green and blue values in small steps, convert them first to CIE-XYZ values and then to CIELAB. We then apply an adaptation of the lightness  $L^*$  values according the desired lightness range mapping function defined by Eq. (1) and establish the concave gamut by Delaunay triangulation and ball-pivoting [7]. The *sRGB* white is mapped to the paper white by taking as CIELAB white reference the display white for

converting *sRGB* values to CIELAB colors and the paper white for converting tri-stimulus values of print samples from CIE-XYZ to CIELAB colors.

Let us show and compare the non-fluorescent  $G_{cm\gamma k}$  gamut comprising only the colors generated with the classical *cm\gamma k* inks, the printable fluorescent  $G_f$  gamut comprising colors generated with the classical inks and the daylight fluorescent magenta and yellow inks and the linearly lightness adapted *sRGB* gamut  $G'_{sRGB}$ .

Under the D65 illuminant, Figure 3a shows in 3D the  $G_{cm\gamma k}$  and the  $G_f$  gamuts. At high lightness values ( $L^* > 60$ ), we observe a gamut extension in the yellow, magenta, red, orange and green parts of the gamut due to the fluorescence of the  $y_f$  and  $m_f$  inks. Figure 3b illustrates a comparison between the printable destination fluorescent gamut  $G_f$  and the linearly lightness adapted  $G'_{sRGB}$  gamut. A significant part of the  $G_f$  gamut is outside the  $G'_{sRGB}$  gamut. We therefore have to propose a suitable mapping from the  $G'_{sRGB}$  gamut to the  $G_f$  gamut that enables expanding the input  $G'_{sRGB}$  gamut colors into the  $G_f$  printable gamut.

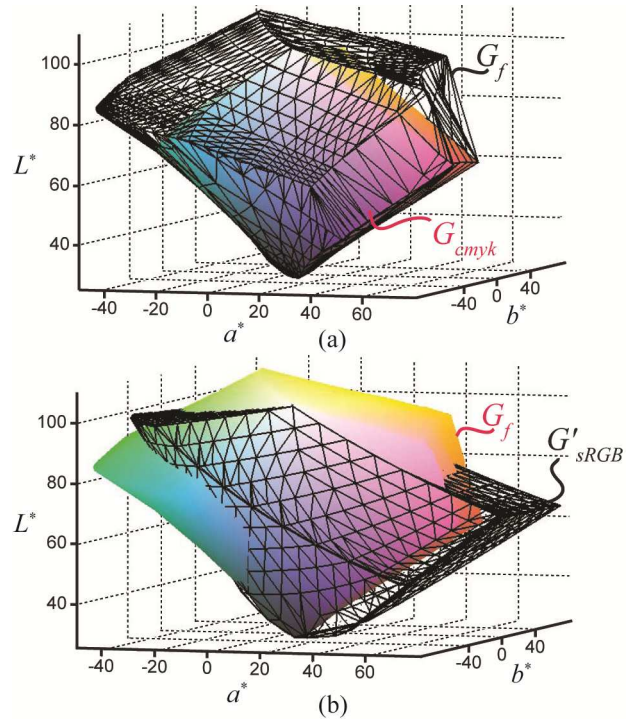


**Figure 3.** (a) Comparison between the gamut  $G_{cm\gamma k}$  (colored solid) and the printable fluorescent ink gamut  $G_f$  (mesh grid) and (b) comparison between the printable fluorescent ink gamut  $G_f$  (colored solid) and the display lightness adapted gamut  $G'_{sRGB}$  (mesh grid).

Let us compute the gain offered by the  $G_f$  gamut in respect to the  $G_{cm\gamma k}$  gamut as well as the volume of colors offered by the  $G_f$  gamut beyond the  $G'_{sRGB}$  gamut (Table 1). By printing image parts with the  $G_f$  gamut, we increase the  $G_{cm\gamma k}$  gamut volume by 56%. We are also able to use 249K  $L^* a^* b^*$  volume units of high brightness and high chroma colors which are not available within the  $G'_{sRGB}$  gamut.

**Table 1. Comparison of gamut volumes (in thousand volume units).**

Gamut volumes	
Volume $G_{cmyk}$	343
Volume $G_f$	537
gain	56%
Lightness adapted volume $G'_{sRGB}$	626
Volume $G_f \subset G'_{sRGB}$	249

**Mapping the lightness adapted sRGB gamut onto the printable fluorescent gamut**

The lightness adapted gamut  $G'_{sRGB}$  is mapped into the printable destination fluorescent gamut according to a multiple foci gamut approach [8], as shown in Figure 4. We define an upper lightness bound  $l_h$  and a lower lightness bound  $l_l$ . For a color point  $C_{source}$  of the source gamut  $G_{source}$ , we apply a mapping from point  $C_{source}$  to  $C_{dest}$  on a line passing through  $C_{source}$  and through the focal point on the black and white axis for  $C_{source}$  color points that have a lightness either  $L_{source} > l_h$  or  $L_{source} < l_l$  or on a constant lightness line passing through  $C_{source}$  when  $l_l \leq L_{source} \leq l_h$  (Fig. 4, pointed lines). The mapping line intersects the source and destination gamut boundaries at respective intersection points  $C_{sourceMax}$  and  $C_{destMax}$ .

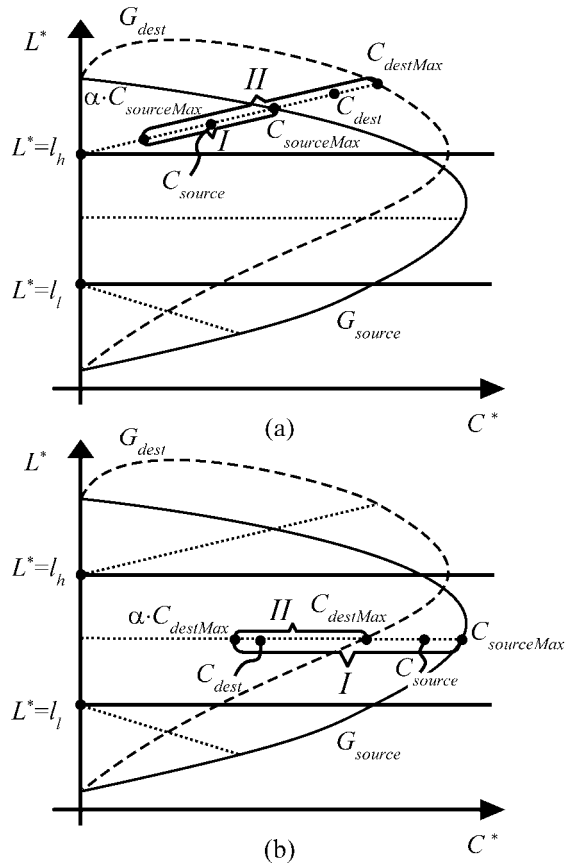


**Figure 4. Multiple foci gamut mapping approach for (a) gamut expansion of point  $C_{source}$  to  $C_{dest}$  and (b) gamut reduction of point  $C_{source}$  to  $C_{dest}$ .**

In case of gamut expansion, i.e.  $C_{destMax} > C_{sourceMax}$  (Figure 4a), we apply a chroma expansion to chroma values  $C_{dest}$  by mapping the interval (I):  $[\alpha \cdot C_{sourceMax}, C_{sourceMax}]$  into the interval (II):  $[\alpha \cdot C_{sourceMax}, C_{destMax}]$  according to the following equation

$$C_{dest} = \alpha \cdot C_{sourceMax} + \left( \frac{C_{source} - \alpha \cdot C_{sourceMax}}{C_{sourceMax} - \alpha \cdot C_{sourceMax}} \right)^\gamma (C_{destMax} - \alpha \cdot C_{sourceMax}) \quad (2)$$

where factor  $\gamma$  expresses a possible non-linearity of the chroma mapping. With  $\gamma = 1$ , the mapping is linear and with  $0 < \gamma < 1$ , chroma is non-linearly expanded. Factor  $\alpha$  between 0 and 1, defines the internal part of the source gamut where chroma values do not change, i.e. within the interval  $0 \leq \alpha \cdot C_{sourceMax}$  we have  $C_{dest} = C_{source}$ . This prevents the chroma increase of low chroma colors.

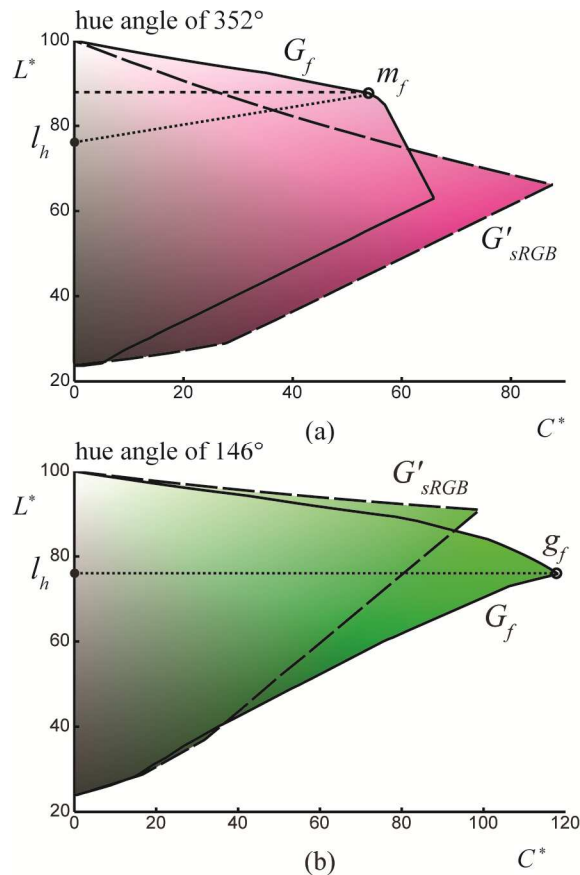


**Figure 5. Constant hue plane (a) at a hue angle of  $352^\circ$  showing both a constant expansion lightness mapping line (dashed line) and a non-constant lightness mapping line (pointed line) in direction of the magenta fluo solid ink ( $m_f$ ) and (b) at a hue angle of  $146^\circ$  showing a constant lightness mapping line (pointed line) in direction of the green fluo colorant ( $g_f$ ).**

Figure 5 illustrates the need of a multiple foci approach for expanding color points. In case of chroma expansion towards the color of a daylight fluorescent colorant, we should avoid mapping a small range of colors into a large range of colors.

For the considered printable fluorescent gamut, we set the upper bound to  $l_h = 76$ . In the hue plane of the  $m_f$  ink, compared with constant lightness mapping (Fig. 5a, dashed line) the non-constant lightness mapping line passing through the  $m_f$  ink color (Fig. 5a, pointed line) maps a significantly larger range of input gamut colors. The non-constant lightness mapping is also required in order to map input colors into the color of the  $y_f$  ink whose maximal lightness is  $L^* = 108$ , i.e. higher than the maximal source gamut lightness at  $L^* = 100$ . For mapping green colors, e.g. at a hue angle of  $147^\circ$ , applying constant lightness mapping in the lightness range  $l_l \leq L^* \leq l_h = 76$  is appropriate since the source range of color is large enough (Fig. 5b, pointed line). In addition, the upper lightness focal point also controls the lightness shift when expanding source colors. For instance, by decreasing the lightness of the focal point  $l_h$ , colors with lightness higher than  $l_h$  are expanded towards higher lightnesses.

In case of gamut reduction, i.e.  $C_{sourceMax} \geq C_{destMax}$  (Fig. 4b), we apply a chroma reduction to chroma values  $C_{dest}$  by mapping the interval (I):  $[\alpha \cdot C_{destMax}, C_{sourceMax}]$  into the interval (II):  $[\alpha \cdot C_{destMax}, C_{destMax}]$  according to the following equation

$$C_{dest} = \alpha \cdot C_{destMax} + \left( \frac{C_{source} - \alpha \cdot C_{destMax}}{C_{sourceMax} - \alpha \cdot C_{destMax}} \right) (C_{destMax} - \alpha \cdot C_{destMax}) \quad (3)$$

The lower lightness bound  $l_l$  used for reducing chroma prevents a too strong chroma reduction in dark tones and therefore better preserves the original image colors.

## User driven gamut expansion

In this section, we define user parameters that enable controlling the gamut expansion. We would like to control the chroma enhancement within image parts selected by users. Within the selected image parts, we apply a gamut expansion of the input image  $sRGB$  colors by mapping the input chroma interval either linearly or non-linearly onto the printable output chroma interval, by considering the maximal chroma or a part of the maximal chroma achievable by the printable fluorescent gamut. In addition, in order to avoid artifacts at the boundary between the expanded and non-expanded image parts, we create smooth chroma transitions from the center of the selected image part reproduced with high chroma colors to the border of the selection reproduced with lower chroma colors. Input  $sRGB$  image colors are mapped according to the equations presented in the previous section with additional user-defined parameters that are described below.

Outside the user selected image parts, no  $sRGB$  gamut expansion is performed. An input  $C_{source}$  color is mapped according to Eq. (3) when  $C_{destMax} \leq C_{sourceMax}$  or when  $C_{destMax} > C_{sourceMax}$  is kept as it is, i.e.  $C_{dest} = C_{source}$ . Within the selected image parts, the lightness adapted  $sRGB$  chroma can be enhanced. We distinguish two cases. The first case is when the destination fluorescent gamut is greater than the source gamut along the mapping line ( $C_{destMax} > C_{sourceMax}$ ). In this case, the chroma can be expanded according to Eq. (2) and possibly with the non-linear expansion factor  $\gamma$  varying within  $0 < \gamma < 1$ . This chroma expansion can be limited according to a user-

defined chroma expansion limitation factor  $\delta$ . This chroma expansion limitation factor limits the effective maximal chroma expansion  $C_{destMaximalExp}$  to values between  $C_{destMax}$  and  $C_{sourceMax}$ . The effective maximal chroma expansion then becomes

$$C_{destMaximalExp} = C_{sourceMax} \cdot \delta + C_{destMax} (1 - \delta) \quad (4)$$

and replaces  $C_{destMax}$  in Eq. (2), for  $0 \leq \delta \leq 1$ . Parts of images reproduced with the maximal expansion limitation factor of  $\delta = 1$  do not contain chroma expanded colors.

The second case is when the source gamut is greater than the destination gamut along the mapping line ( $C_{sourceMax} > C_{destMax}$ ). In this case, the chroma of a  $C_{source}$  color can be reinforced by non-linearly increasing the source  $C_{source}$  chroma towards the chroma  $C_{sourceMax}$  with the non-linear chroma expansion factor  $\gamma$  as follows

$$C_{sourceExp} = \alpha \cdot C_{destMax} + \left( \frac{C_{source} - \alpha \cdot C_{destMax}}{C_{sourceMax} - \alpha \cdot C_{destMax}} \right)^\gamma (C_{sourceMax} - \alpha \cdot C_{destMax}) \quad (5)$$

and then performing the gamut reduction  $C_{sourceExp}$  to  $C_{dest}$  according to Eq. (3) by replacing  $C_{source}$  with  $C_{sourceExp}$ . This yields a reinforced chroma color  $C_{dest}$  within the printable fluorescent gamut. By using the same chroma expansion factor  $\gamma$  in both the chroma expandable and the non-expandable parts of the input gamut, we ensure the continuity of the mapped colors. The two user parameters  $\delta$  and  $\gamma$  respectively limit the maximal gamut expansion and provide a non-linear increase of the chroma.

In order to suppress strong chroma differences at the boundaries between selected and non-selected image parts, we create smooth chroma transitions at the proximity of the boundaries of the selected image parts. For this purpose, we establish a spatial interpolation map with values varying between 1 and 0. The final colors are obtained by interpolation between the gamut mapped colors  $C_{destExp}$  with user-defined  $\gamma$  and  $\delta$  parameters and the non-expanded destination colors  $C_{destNonExp}$  located outside the selected image parts.

$$C'_{dest} = C_{destExp} \cdot \Delta(x, y) + C_{destNonExp} (1 - \Delta(x, y)) \quad (6)$$

where the  $\Delta$  values are given by the spatially laid out interpolation map. With  $\Delta = 1$ ,  $C'_{dest}$  represents the user-defined gamut expanded colors and with  $\Delta = 0$ ,  $C'_{dest}$  represents the non-expanded colors located outside the selected image parts. The spatial interpolation map is created with the distance transform algorithm [12]. Pixels outside the user selected image part are set to black and inside the selection to white. We then apply the distance transform to obtain for each white pixel its distance to the nearest black pixel. This distance map is normalized by dividing its values by its maximal value. In order to limit the distance from the boundary where the interpolation is performed, we multiply the map with a distance limiting factor  $\kappa$  ( $1 < \kappa$ ). Values of the map greater than one are set to 1. Figure 6 shows the generated spatially laid out interpolation map for an arbitrary selection (red line) when using a distance limitation factor  $\kappa = 2.5$ .



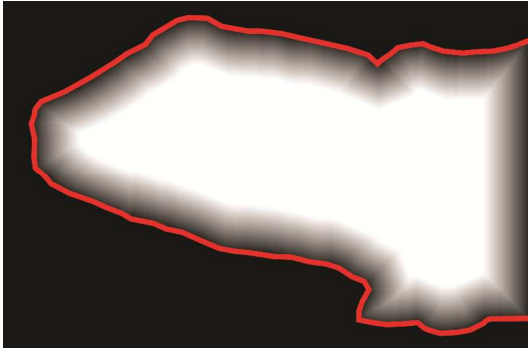


**Figure 6.** Spatial interpolation map for an arbitrary selection (red line) generated with a distance limitation factor  $\kappa = 2.5$ , where white represents 1 and black represents 0.

By spatially interpolating colors between non-expanded colors  $C_{destNonExp}$  and expanded colors  $C_{destExp}$ , we create smooth chroma transitions along the boundaries of the selected image parts.

### Display preview

We developed a tool for designers enabling selecting image parts, applying to these selections the user-defined gamut expansion parameters described in the previous section and previewing the printable destination gamut expanded image. In order to display the chroma expanded image parts, we need to show on a *sRGB* display colors located beyond the original display gamut. With to goal of both preserving the overall appearance of the destination image and observing the differences between the expanded and non-expanded image colors, we simulate on a standard *sRGB* display a display having lower tri-stimulus phosphor values. This simulated lower luminance display renders the non-expanded colors as well as the expanded colors.

Printable gamut mapped CIELAB values that are to be previewed are transformed into CIE-XYZ tri-stimulus values  $XYZ_{printable}$ . We then apply to the  $XYZ_{printable}$  values a multiplicative tri-stimulus reduction factor  $\varepsilon$  ( $0 \leq \varepsilon \leq 1$ ) and obtain the simulated  $XYZ_{sim}$  values. The simulated  $XYZ_{sim}$  values are then transformed to display *sRGB* values and displayed.

The system (or the user) can modify the tri-stimulus reduction  $\varepsilon$  factor until no displayed values saturates the *sRGB* display Red, Green and Blue channels. By assuming that the eye adapts on the simulated  $\varepsilon \cdot X_n Y_n Z_n$  white reference, it becomes possible to visualize the selected gamut expanded image parts. Since the maximal lightness and respectively maximal chroma producible with the 6 ink print setup is  $L^* = 108$  respectively  $C^* = 123$ , values of the tri-stimulus reduction factor  $\varepsilon$  are above 0.7.

### Halftoning and printing

For printing an input *sRGB* image mapped according to user-defined gamut mapping parameters, we have to generate the 6 ink separation layers containing the ink surface coverages of the classical *cmYk* inks and the additional daylight fluorescent magenta and yellow inks. These separation layers

are obtained by establishing a relationship between ink surface coverages and mapped CIELAB values. In a first step, we create a uniform CIELAB grid within the destination fluorescent gamut and fit the surface coverages of the CIELAB grid color points by performing a gradient descent on the ink spreading enhanced cellular Yule-Nielsen spectral Neugebauer model. Then, for each input *sRGB* gamut mapped color that is to be printed, we apply a 3 dimensional lookup table based interpolation [13] between computed surface coverages of CIELAB grid. The details of the algorithm are given in [2].

### Results

Figure 7a shows a photograph of the print preview of a lizard where the selection comprising the animal and its boundaries has been gamut expanded with a non-linear expansion factor  $\gamma = 0.3$  and with smooth chroma transitions between the gamut expanded and outer non-gamut expanded parts. The corresponding spatial interpolation map using a distance limitation factor  $\kappa = 2.5$  is shown in Figure 6. In addition, in order to render out of *sRGB* printable gamut colors, a tri-stimulus display reduction factor of  $\varepsilon = 0.88$  has been applied. Figure 7b shows a photograph of the corresponding printed image and Figure 7c shows a photograph of the same lizard image printed without any chroma expansion with classical *cmYk* inks only. The images were printed with an Epson P50 printer with original Epson *cmYk* inks and with the daylight fluorescent yellow ink (Farbel Castel ink ref. 154907) and the daylight fluorescent magenta ink (Farbel Castel ink ref. 154928). Digital pictures of the prints as well as the previewed print were taken with a Canon PowerShot S95 camera under normal daylight conditions.

By comparing the printed gamut expanded image (Fig. 7b) with its corresponding display preview (Fig. 7a), we observe that the non-expanded part of the image have similar colors both in the preview and in the print. However, the gamut expanded part within the head of the lizard have different colors, i.e. in the photograph, the print colors appear brighter and less saturated. This is mainly due to the fact that colors of the print within the selected image part are beyond *sRGB* colors and can therefore not be rendered with an *sRGB* image captured by a digital camera. Finally, by comparing the printed gamut expanded image with a classical *cmYk* print of that image (Fig. 7c), we observe that within the selected image parts colors are brighter and have a higher chroma. In Figure 7b, since the  $G_f$  gamut covers a larger part of the  $G_{sRGB}$  gamut compared with  $G_{cmYk}$  gamut coverage, the image parts outside the selection where no chroma expansion has been applied are also better reproduced. For example, in the printed fluorescent ink image, the stone colors match the original *sRGB* image while the stone colors in the *cmYk* printed image (Fig. 7c) do not match the original *sRGB* stone colors.

Figure 8 shows photographs of the Rolex Yachtmaster watch advertising image (a) non gamut-expanded and printed with classical *cmYk* inks and (b) the same image with the watch being gamut expanded with a non-linear chroma expansion factor of  $\gamma = 0.3$ . By expanding the chroma of the watch colors, we increase the attention of the observer. By comparing the sailor in both prints, we observe that even without being gamut

expanded, the face and hair of the sailor are better rendered and have a higher contrast with the  $G_f$  gamut (Fig. 8b) than with the  $G_{cmyk}$  gamut (Fig. 8a). They better preserve the original Yachtmaster advertising image.



(a)



(b)



(c)

**Figure 7.** Photographs of (a) the display preview of a lizard image where a selection comprising the lizard as well as its boundary pixels has been gamut expanded and where smooth chroma transitions have been created between the inner and outer parts of the selection, (b) the image printed with fluorescent and classical inks and (c) the classical cmyk print of the lizard image. Please observe the images on the electronic version of this article.



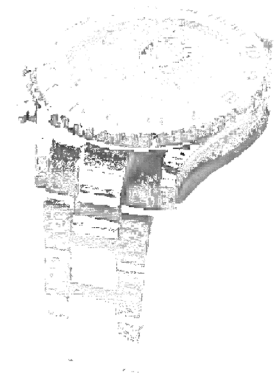
(a)

(b)

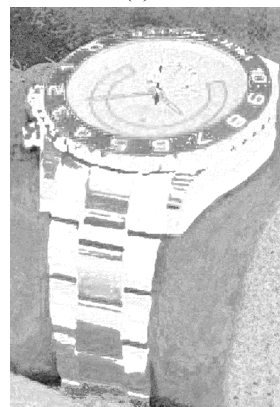
**Figure 8.** Photographs of a printed (a) non-expanded Rolex Yachtmaster image with the classical  $G_{cmyk}$  gamut and (b) of the same image printed with the  $G_f$  gamut, where a selection comprising the watch is gamut expanded with a non-linear expansion factor  $\gamma = 0.3$ . Please observe the images on the electronic version of this article.



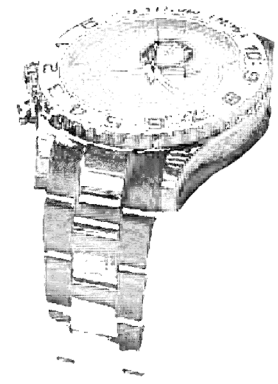
(a)



(b)



(c)



(d)

**Figure 9.** The yellow (a), daylight fluorescent yellow (b), magenta (c) and daylight fluorescent magenta (d) ink layers of the gamut expanded Rolex Yachtmaster watch image. Layers are shown in grayscale with the darkness of each pixel representing the ink surface coverage.

For the watch shown in Figure 8b, Figure 9 represents the  $y$ ,  $y_f$ ,  $m$  and  $m_f$  ink layers in grayscale. The darkness of each pixel represents the ink surface coverage. A significant part of the watch has been reproduced with the  $m_f$  and  $y_f$  inks. This yields the brighter and higher chroma colors of the watch shown in Figure 8b.

## Conclusion

We propose a framework for expanding the colors of *sRGB* images towards printable high chroma and bright colors located beyond display *sRGB* gamut colors. High chroma and bright colors are obtained by performing a gamut expansion of the original image gamut onto the gamut covered by the combined *cmYk* and the magenta and yellow fluorescent inks. Fluorescent ink halftones add a new dimension to color prints. They enable highlighting specific image parts which then attract the attention of the observer. Applications include the design of posters and images for advertisement. The proposed color reproduction framework enables users to choose (a) the image regions to be enhanced, (b) how far the chroma should be expanded and (c) the possible non-linearity of the chroma expansion. Users can display a preview of the gamut expanded image print. This is useful for designers working in fields such as photography, advertisement and production of magazines as well for artists who wants to create new print effects. Future work should include studies about the extent to which chroma expansion of prints improves the communication of its embedded message.

## Acknowledgement

The authors express their gratitude to Sergiu Gaman who programmed the preview software. We also thank the Swiss National Science Foundation for their support, grant n° 200020-126757/1.

## References

- [1] Karl Guyler, Visualization of expanded printing gamuts using 3-dimensional convex hulls, *American Ink Maker*, 79(9):36–56, September 2001.
- [2] R. Rossier, R.D. Hersch, Reproducing color images by combining classical and daylight fluorescent inks, submitted to the *IEEE Transactions on Image Processing*.
- [3] E. J. Stollnitz, V. Ostromoukhov, and D. H. Salesin. Reproducing color images using custom inks. In *Proceedings of SIGGRAPH 98*, pages 267-274. ACM, New York, 1998.
- [4] D. Tzeng, R.S. Berns, Spectral-based six color separation minimizing metamerism, *IS&T/SID 8th Color Imaging Conference*, pp. 342-347.
- [5] F. Grum, Colorimetry of fluorescent materials, in *Optical Radiation Measurements, Volume 2, Color Measurements*, F. Grum and C. J. Bartelson, eds. (Academic, 1980), pp. 235–288.
- [6] R. Rossier, R.D. Hersch, Introducing ink spreading within the cellular Yule-Nielsen modified Neugebauer model, *Proc. IS&T/SID's 18th Color Imaging Conference*, pp. 295-300, 2010.
- [7] F. Bernardini, J. Mittleman, H. Rushmeier, C. Silva, and G. Taubin, The Ball-Pivoting Algorithm for Surface Reconstruction, *IEEE Trans. Visualization and Computer Graphics*, vol. 5, no. 4, pp. 349-359, Oct.-Dec. 1999.
- [8] J. Morovic, M. R. Luo, The fundamentals of gamut mapping: A survey, *J. Imag. Sci. Technol.*, vol. 45, no. 3, pp. 283–290, 2001.
- [9] S. G. Streitel, *Fluorescent Pigments (Daylight)*. Kirk-Othmer Encyclopedia of Chemical Technology. 2009. 1–25.
- [10] S.A. Connors-Rowe, H.R. Morris, P.M. Whitmore, Evaluation of appearance and fading of daylight fluorescent watercolors, *J. Am. Inst. Conserv.*, 2005, pp. 44, 75-94.
- [11] Byoung-Ho Kang, Jan Morovic, M. Ronnier Luo, and Maeng-Sub Cho, Gamut Compression and Extension Algorithms Based on Observer Experimental Data, *ETRI Journal*, Vol. 25, no. 3, pp.156-170, 2003.
- [12] Rosenfeld A, Pfaltz J. L., Distance functions on digital pictures, *In Pattern Recognition*, 1(1):33-61, 1968.
- [13] Henry R. Kang, Chapter 9, Three-Dimensional Lookup Table with Interpolation, In *Computational Color Technology*, Vol. PM159 (17 May 2006), pp. 151-159.
- [14] T. Hirokawa, M. Inui, T. Morioka, and Y. Azuma. A psychophysical evaluation of a gamut expansion algorithm based on chroma mapping ii: Expansion within object color data bases. *NIP23*, pages 175–179, 2007.

## Author Biography

Romain Rossier is PhD student at the Peripheral Systems laboratory (Ecole Polytechnique Fédérale de Lausanne, or EPFL) in Lausanne, Switzerland. His research interests include color prediction, mathematical modeling of printing processes, color printing with inkjet and optical document security. He obtained his master degree in computer science from EPFL in 2007. He received the MERL Best Student Paper Award at the IS&T/SID 19th Color and Imaging Conference (CIC), San Jose, CA, Nov. 2011 for his paper "Hiding Patterns with Daylight Fluorescent Inks". He is author and co-inventor in US patent applications.